STRESS RELAXATION IN Fe - B - Si METALLIC GLASS RIBBONS

A Thesis Submitted
in Partial Fulfilment of the Requirements
for the Degree of

MASTER OF TECHNOLOGY

By
R. SRIDHAR

to the

INTERDISCIPLINARY PROGRAMME IN MATERIALS SCIENCE

INDIAN INSTITUTE OF TECHNOLOGY KANPUR

AUGUST, 1983

To

My Parents

C E R T I F I C A T E

This is to certify that this thesis entitled 'Stress relaxation in Fe-B-Si Metallic glasses ribbons' submitted in partial fulfilment of the requirements for the Degree of Master of Technology by Mr. R. Sridhar, is a record of work carried under my supervision and has not been submitted elsewhere for a degree.

D.C. Agrawal
Assistant Professor
Materials Science Programme
I.I.T. Kanpur

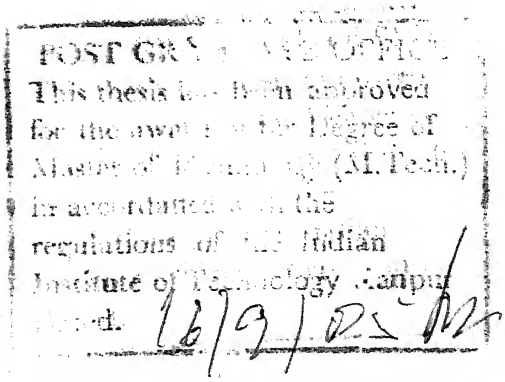

A C K N O W L E D G E M E N T

I sincerely thank Dr. D.C. Agrawal for his valuable guidance and encouragement throughout this work. Many useful discussions with him regarding this work are gratefully acknowledged.

I owe my thanks to Dr. K.P. Gupta for allowing me to use the arc furnace and Dr. Sanjay Gupta for permitting me to use the mini-computer in A.C.M.S. I am grateful to Mr. B.K. Jain for the help rendered during the experimental work and for making excellent drawings at such a short notice. My sincere thanks are due to Mr. R. Venkatesh for helping me in writing the computer programs, Mr. S. Murugan, Mr. R. Gopalakrishnan, Mr. R. Sundar Rajan and Mr. R. Palaniswamy for helping me during the typing and the correction of this thesis work.

I thank Mr. S.R. Bhardwaj for his excellent typing. Finally I thank all the technical staff of ACMS and my friends for their co-operation and help whenever needed.

CONTENTS

LIST OF FIGURES

A B S T R A C T

Stress relaxation in Fe-B-Si metallic glasses has been studied by tensile and Bend stress relaxation techniques. The data have been analyzed to yield strain rate sensitivity, change in viscosity with time and rate of change of viscosity at different temperatures. The extent of stress relaxation in the three compositions studied is found to increase in the order $Fe_{75.8}\ B_{17.4}\ Si_{6.8}$ $<$ $Fe_{80.3}\ B_{12.4}\ Si_{7.3}$ $<$ $Fe_{80.2}\ B_{14.9}\ Si_{4.9}$ while the rate of viscosity increase at a temperature follows the reverse order. The strain rate sensitivity index $m = \dfrac{d \ln \dot{\gamma}}{d \ln \tau}$ is found to be nearly one for intermediate stress levels and more than 2 for high stresses. The composition dependence of the stress relaxation follows the trend reported in literature.

CHAPTER - I

INTRODUCTION

Metallic Glasses drew wide attention among material scientists when Klement, Williens and Duwez [1] in 1960 reported that a liquid Au-Si alloy, when rapidly quenched to liquid nitrogen temperature, would form an amorphous solid. Prior to this, amorphous metals had been prepared by both vapor diposition [2] and electro-deposition [3] techniques but only after 1960, research activities were increased in this field. A large number of different alloys have been produced as metallic glasses and their structure related properties, mechanical behaviour and magnetic properties have been studied and reviewed extensively. [4-6]

Amorphous Solids in effect constitute a totally new class of materials with physical propetties which are different form those of crystalline alloys. For example, though the metallic glasses are as dense as the Crystalline materials [7] they posses random structures similar to those of the corresponding liquids. Their structures are homogeneous both microscopically and macroscopically and they posses none of the microstructural features that resemble those of the crystalline materials. Though these properties are of basic scientific interest, they also posses various properties that are interesting

to technologists like very high strength and hardness [8,9] very good magnetic properties like high permeablity and low losses [10] and superior corrosion resistance properties [11] These properties make them potentially very useful technological materials.

If a liquid metal is splat cooled sufficiently fast to avoid Crystallization, its viscosity increases rapidly until a temperature is reached at which the configuration of the super cooled liquid is "frozen in "to form a metallic glass. The exact " frozen in " structure depends upon the cooling rate during the formation of the glass [12]. The as-quenched glasses have a highly disordered structure which is metastable not only with respect to the equalibrium crystalline phase but with respect to a more stable glass. Consequently on subsequent annealing the glass, will first lower its energy by relaxing to a more stable glassy state and at high temperatures it will crystallize. During this low-temperature structural relaxation, significant and useful changes in magnetic properties [13], thermal conductivity [14], Creep [15-18] and in viscous flow [19,20] occur. These changes can be attributed to atomic rearrangements during structural relaxation. Though the precise atomistic movements are unknown, they may be of two distinct seperable types [21]. changes in topological short range order (TSRO) that involves largely the elimination and redistribution of free-whome and charges in compositional short range order (CSRO) i.e. in nearest neighbour atom pairs.

Stress relaxation of metallic glasses is briefly reviewed in Chapter II. The metallic glass ribbons, used in this study, were produced by chill block melt spinning method [22]. Two types of stress relaxation tests were performed. Tensile stress relaxation tests were performed on an Instron Universal testing machine with a specially designed fixture. Bend stress relaxation tests were carried out by constraining the metallic glass ribbons to different initial radii during annealing. Stress relaxed samples were analysed by diffrential scanning calorimetry. Results of these experiments are discussed in chapter IV. Summary of the work and the conclusions that can be drawn are presented Chapter V.

CHAPTER - II

STRESS RELAXATION BEHAVIOUR

Stress relaxation behaviour of metallic glasses is briefly reviewed. The differences between homogeneous and inhomogeneous flow will be discussed in the first section. This is followed by the discussion about controversies in the measured values of strain rate sensitivity. Transition state theory and threshold stresses applicable to flow processes are discussed in the final section.

II.1 Flow mechanisms in Metallic Glasses.

There are basically two modes of deformation in uniaxial tension for the metallic glasses. (a) Homogeneous Flow (b) Inhomogeneous Flow the characteristics of the both the flows are briefly described here.

II. 1.1 Homogeneous Flows in Metallic Glasses.

In this mode of deformation, each volume element of the specimen contributes to the strain. In a uniaxial tensile test, specimen thins down uniformly during deformation. Fracture occur at large strains i.e. at excessive plastic flow when the thickness in some part of the specimen has narrowed down tozero value. This flow mechanism operates at low stress levels at all the temperatures and except near the boundary of the inhomogeneous deformation, is almost always

Newtonion-viscous i.e. $\dot{\gamma} \propto \tau$. The region of homogeneous deformation can be subdivided according to the temperature of the ribbon, into three regions which are defined somewhat arbitarily.

(a) $T > T_l$. T_l is the melting point of the liquid. Metallic Glass ribbons can be characterized as 'fluid' in this region and has a viscosity $\eta = 10^{-3}$ Nm^{-2} sec. Only one set of viscometric measurements on the glass forming melt has been reported [23] Viscosity was observed to slowly increase with temperature.

(b) $T \simeq T_g$ (glass transition temperature). Viscosity isby definition approximately equal to 10^{10} to 10^{15} Ns/m^2 in this region and hence the system could be called as viscous. In this region number of creep-type viscosity measurements have been reported [23,24,25].

In this temperature range it is possible to evaluate the viscosity from a set of colorimetrically obtained glass transition and stress relaxation data. In this region the viscosity falls very steeply with the increasing temperatures [19,20].

C. $T < T_g$. The material has a viscosity around 10^{15} N/m^2 sec. and it can be called a solid. Creep measurements in this region are complicated by continious structural relaxation of the system towards higher viscosities.

This resulted in different values of strain rate

sensitivity index. Strain rate sensitivity index reported by Hadnagy et. al. [18] is grater than the values reported by Maddin and Masumoto [15,16] but is similar to Megusar's recent observations [26].

II.1.2 Inhomogeneous Flow in Metallic Glasses.

This mode of deformation occurs at high stress region in which stress is very strain rate insensitive i.e. $m = \frac{\partial \log \dot{\gamma}}{\partial \log \tau}$ is very large so that the flow is ideally plastic. The flow stress at a given strain rate, when normalized by the shear modulus which is temperature dependent is almost constant with temperature except near Tg. In this inhomogeneous deformation, the strain is localized in a few very thin shear bands. If ribbons pulled in tension, these shear bands are planes usually perpendicular to the thin side of the ribbon and at a 45° angle with the tensile load axis [27,28,29]

This weakens the specimen locally by decreasing the corss-section, until finally fracture occurs along to planes of those shear bands [28,30].

II. 2. Application of transition state theory to the flow processes.

II.2.1. Controversies in the reported measurements of creep and stress relaxation data.

While analyzing the results of the creep and stress relaxation experiments, two distinct types of behaviours are observed

(a) At low stresses, Newtonions behaviour was observed [15,19, 32] i.e. strain rate is proportional to the stress $\sigma = \eta\dot{\varepsilon}$ where η is the viscosity.

The strain rate sensitivity index m which is defined as $m = \dfrac{d \log \dot{\gamma}}{d \log \tau}$ is equal to unity.

(b) At higher stresses, power law of creep namely $\sigma = A\dot{\varepsilon}^m$ was observed [18,33] A is a constant and m depends on stress. When various experiments on stress relaxation and creep are compared, discrepencies in the reported values of m are found. [15, 17-20, 26] . Strainrate sensitivity index m is expected to be linear at low stresses and expected to increase with stress at high stresses [37].

But in one set of tensile stress experiments were conducted over a large range of stress, m was found to increase dramatically with stress and a maximum value of 12 is reported [26]. In another experiment over the same stress ranges, value of m is reported to be constant and equal to 4. [18,36] To avoid these discrepencies, the transitionstate theory was applied to the flow processes and a expression for strain rate interns of the stress is derived.

II.2.2 Flow equation for stress relaxation experiment.

Two flow models were proposed on the basis of transition state theory. Plastic flow is assumed to take place as a

result of dynamic equalibrium between the stress biased creation and diffusional annhilation of the structural disorder. The resulting shear strain rate $\dot{\gamma}$ is expressed as a function of the hyperbolic sine term that contains the shear stress and the atomic volume [38]. Second model is based on the thermally activated shear transformations initiated around free volume regions with the shear strain rate expressed interms of the hyperbolic sine functions [39]. The flow equation for the later case can be derived as follows [40].

Consider a strain producing element in terms of its free energy diagram as shown in Fig. II.1. Let Ω_f be the volume of stable local atomic configuration, which is situated in a local free energy minimum. When the applied shear stress is equal to 0, flow will occur whenever the thermal energy kT exceeds the activation barrier. According to the Maxwell - Bolftzman's statistics number of forward shear flow events N_f is equal to number of backward flow events N_b.

$N_f = N_b = p_c \exp(-\Delta G^*/kT)$ .....II.3 where p_c is the probability of shear flow taking place in that configuration and ΔG is the activation energy.

Because of the applied shear stress, work done by the flow lowers the free energy in the forward direction and increases the free energy inthe backward flow direction by an amount equal to $\frac{\tau \gamma_0 \Omega_f}{2}$. γ_0 is the equivalent shear

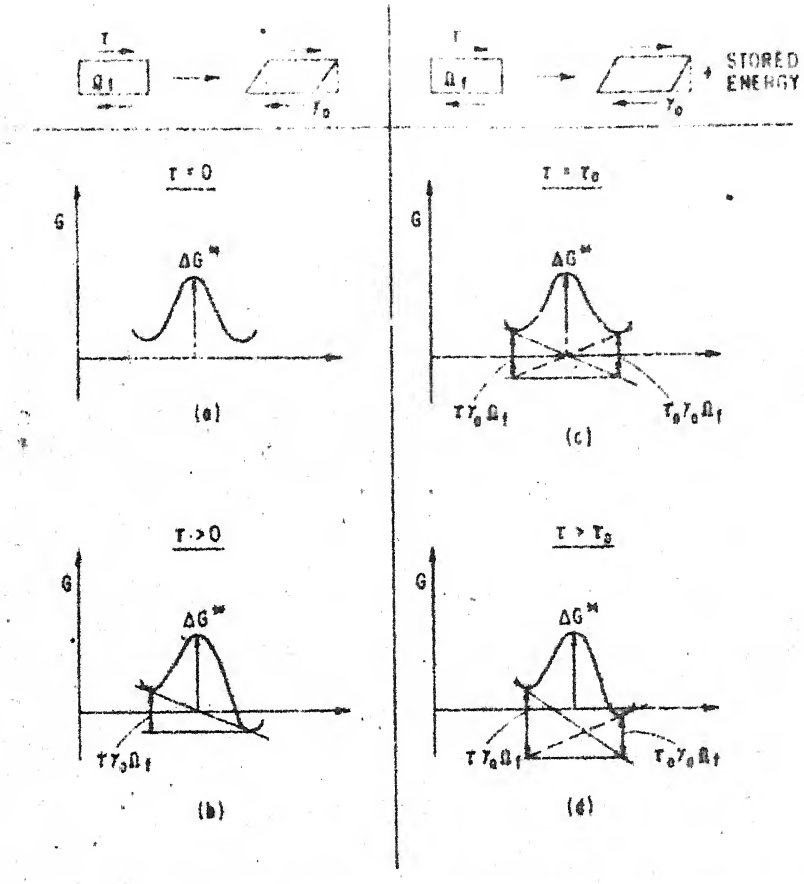

Fig. II.1 Schematic free energy diagrams of local shear flow events, for the case of pure shear work only (a,b) and for the case where the shear work is accompanied by and internal energy increase due to flow induced disordering (c,d). The shear work $\tau\gamma_0\Omega_f$ is shown by the solid line. The stored internal energy $\tau_0\gamma_0\Omega_f$ is illustrated by the dashed line.

strain . The net number of forward jumps is given by

$$2p_c \gamma \exp\left(\frac{-\Delta G^*}{kT}\right) \sin h \left(\frac{\tau \gamma_o \Omega_f}{2\,kT}\right) \quad \ldots \text{ II.IV.}$$

If we take $2p_c \gamma \exp\left(\frac{-\Delta G^*}{kT}\right)$ as $\dot{\gamma}_o$, then the shear strain rate is given by $\dot{\gamma} = \dot{\gamma}_o \sin h \left(\frac{\tau \gamma_o \Omega_f}{2kT}\right)$ ...II.5

The above equation statisfies the stress-strain rate behaviour in the intermediate region and at higher stress regions. In the Intermediate region, $\frac{\tau \gamma_o \Omega_f}{2kT} < 1$ and hence

$$\sin h \frac{\tau \gamma_o \Omega_f}{2kT} \simeq \frac{\tau \gamma_o \Omega_f}{2kT} \quad \ldots\ldots\ldots \text{II.6.}$$

Hence a linear behaviour was expected with strain rate sensitivity index $\simeq 1$. For higher stress, sin h equation fits very well predicting that m increases with stress γ_o is the shear strain produced by the volume Ω_f. One draw back in this equation is that the atomic volume can not be calculated seperately and only the collective value of $\gamma_o \Omega_f$ can be obtained . Ω_f is sometimes calculated on the assumption of unit strain i.e. $\gamma_o = 1$. [41]

II. 2.3 Threshold stresses.

But for very low shear stress it was reported that the strain rate sensitivity index has values > 1. It was found to increase with stress and a non-linear behaviour of stress -

strain rate was observed. This was explained by introducing threshold stress τ_o in the equation II. 6, with $\tau - \tau_o$ replacing τ. In terms of free energy diagram shown in fig. II.1 [c. and d], it was assumed that each atomic flow besides doing work, also increases the internal energy. When the applied stress is equal to the threshold stress the internal energy due to threshold stress is compensated by the work done by the shear flow and hence the free energy is unbiased. When the applied stress is greater than the threshold stress work done is much more than the internal energy and hence there is a decrease in the free energy in the forward shear direction. The decrease in free energy in the forward direction which is equal to the increase in the free energy in the backward shear direction is given by $\Delta G^* - \frac{(\tau - \tau_o)\gamma_o \Omega_f}{2\,kT}$.

So now the flow equation is stated as follows.

$$\dot{\gamma} = \dot{\gamma}_o \sinh\left(\frac{(\tau - \tau_o)\gamma_o \Omega_f}{2kT}\right) \quad \cdots \text{II.7}$$

$\gamma_o \Omega_f$ and τ_o are observed to decrease with time because of the reduction in size of the atomic region participating in the flow event rate and the magnitude of the resulting shear strain γ_o. This reduces the amount of flow. A small strain of small volume disturbs the atomic configuration to a lesser degree than correspondingly larger values.

Disruption in order associated with each flow is smaller and this is manifested in a decrease in τ_o . Both γ_o Ω_f and τ_o decrease with temperature but the exact reasons for this behaviour are not known.

II.3 General Emperical law for the homogeneous flow.

It is possible to propose a general emperical law describing homogeneous flow for several palladium and iron - based amorphous alloys. The proposed equation should contain (a) temperature dependence of iso-configurational flow (b) Stress dependence of the iso configurational strain rate and (c) effect of structural change in the flow rate of amorphous alloys.

For temperatures $T \leq Tg-50$ an Arrhenius-type temperature dependence has been observed [32, 42-46] with an activation energy Q_{iso} that is independent of the stress and the time history of the alloy. The value of Qiso does depend on composition. Activation energy increases with temperature near glass transition temperature [47]. But most of the experiments have been conducted where Qiso remained as constant.

Stress-strain rate relation, as discussed earlier is a hyperbolic relation with stress values incorporated. Volume strains element Ω_f and threshold stress appear to be strongly temperature [48,49] and composition [40,50,51] dependent . Also these parameters change as the structure relaxes [52] but for iso configurational state they will be taken as

a constant and equal to saturation values.

Effect of structural changes on the flow rate is expressed in terms of its viscosity $\eta = \tau/\dot{\gamma}$. It has been shown that viscosity increases dramatically as a consequence of struct structural relaxation in amorphous alloys toward the ideal glassy state [40,46,51,53-55] In allcases rate of viscosity increase is nearly linear. The rate of viscosity increase η is dependent on both temperature and composition but appears to be independent of stresses above the threshold value [16, 56].

By incorporating all these relationships, to general emperical law derived as follows [57]

$$\dot{\gamma}(\tau,T,M) \propto \exp\left\{\frac{Q_{ISO}(T,M)}{KT}\right\} \sinh\left\{\frac{\gamma_0 \Omega_f(T,M)(\tau - \tau_0(T,M))}{2KT}\right\}^{+} \Big/ \eta_0(T,M)+\eta(T,M)\, t^n \quad \ldots (1)$$

Though this model explains the structural relaxation and flow properties, because of limited data, these assumptions can not be verified.

+ In the above equation, the symbols t, τ, T and M which are put in the brackets of the homogeneous flow parameters, represent the depend of these parameters on time, stress, temperature and composition respectively. The viscosity term in the denominator comprises of two factors. Time independant initial viscosity η_0 and time dependant viscosity. $\dot{\eta}$. Dependance on time is controlled by the exponent n.

CHAPTER - III

EXPERIMENTAL WORK

III.1 Fabrication of amorphous metallic glass ribbons.

Chill block melt spinning technique was employed in the fabrication of metallic glass ribbons. The details, of the Fabrication of metallic glasses, fabrication parameters and the experimental arrangement are discussed by E.A. Chakachery [22]. In this technique, a stream of molten metal is directed on a rapidly moving substrate which acts as a continious chill block and as a means for material transport away from the melt. A ribbon is formed by attenuation and solidification of the melt puddle on the substrate. This process is characterized by high linear rates, large volometric through put and high quench rates.

Iron-Boron-Silicon system is chosen for the present study due to the following reasons. Sofar stress relaxation experiments have been carried out on Fe-Ni-P-B and Pd-Si systems. Fe-B-Si metallic glass ribbons are very good magnetic materials with high curie temperature and high saturation magnetization values.[58,59] They are easy glass formers and corrosion resistent[60] since structural relaxation is known to affect these magnetic properties, the relaxation behaviour of these materials is important.

All the materials used in the fabrication of metallic glass ribbons were obtained from Alfa Ventron Company.

A master alloy of Fe-B was made in the arc furnace with composition $Fe_{75}B_{25}$. To this alloy, required amounts of iron and Silicon were added. The Three compositions used in the study are

(a) $Fe_{80.2}$ $B_{14.9}$ $Si_{4.9}$ (b) $Fe_{80.3}$ $B_{12.4}$ $Si_{7.3}$

(c) $Fe_{75.8}$ $B_{17.4}$ $Si_{6.8}$.

These compositions are known to be right in the middle of the amrophous range for the FeBSi system [61]. Typical weight of material used in each ron was 3.5g. This quantity of alloy was kept in a fused silica tube and heated by an induction furnace. The tube was flushed with purified argon gas and then evacuated successively for a minimum of three times both during the initial melting of the alloy for homogenisation and during the ejection of the ribbons and a weak argon gas pressure was maintained through out the melting. The molten alloy was ejected through the nozzle in the silica tube by a argon pressure of the order of 2.0-2.5 kg/cm^2. These ribbons, thus fabricated were found to be amrophous by Transmission Electron Microscopy and by X-ray diffraction techniques.

III.2 Tensile stress relaxation experiment.

Tensile stress relaxation tests were carried out on an model 1194 Instron Universal testing machine. An

experimental arrangement was specially designed for this purpose and is shown in figure III.1. One end of a mild steel bar is connected to the load cell while the other end is made to pass through the hole in the centre of the cross head of the machine and is connected to the upper grip through a pin. Both the pins and the grips were made of stainless steel in order to minimize the expansion of the grips at the test temperature. A circular plate holding the bottem grip is connected to the cross head by means of four vertical mild steel rods. Both the upper and lower grips alongwith two thirds of the length of the mild steel rods were immersed in a Silicone oil bath which can be raised or lowered by means of a jack. The oil bath is surrounded by a heating mantle. The temperature of this heating mantle is controlled by a temperature controller which controls the temperature within $\pm$ 1°C. The edges of the stainless steel grips were ground so as to avoid stress concentrations taking place at the edges of the grips.

III.3 Typical run.

Metallic Glass ribbons of 7.5cm length were used in the experiments. The edges of the ribbons were smoothered as for as possible by polishing them which minimized the irregularities in the edges and the nearly uniform width was achieved. The width of the ribbons were measured by a travelling microscope. Thickness of the ribbons were measured using a Mitutoyo micrometer.

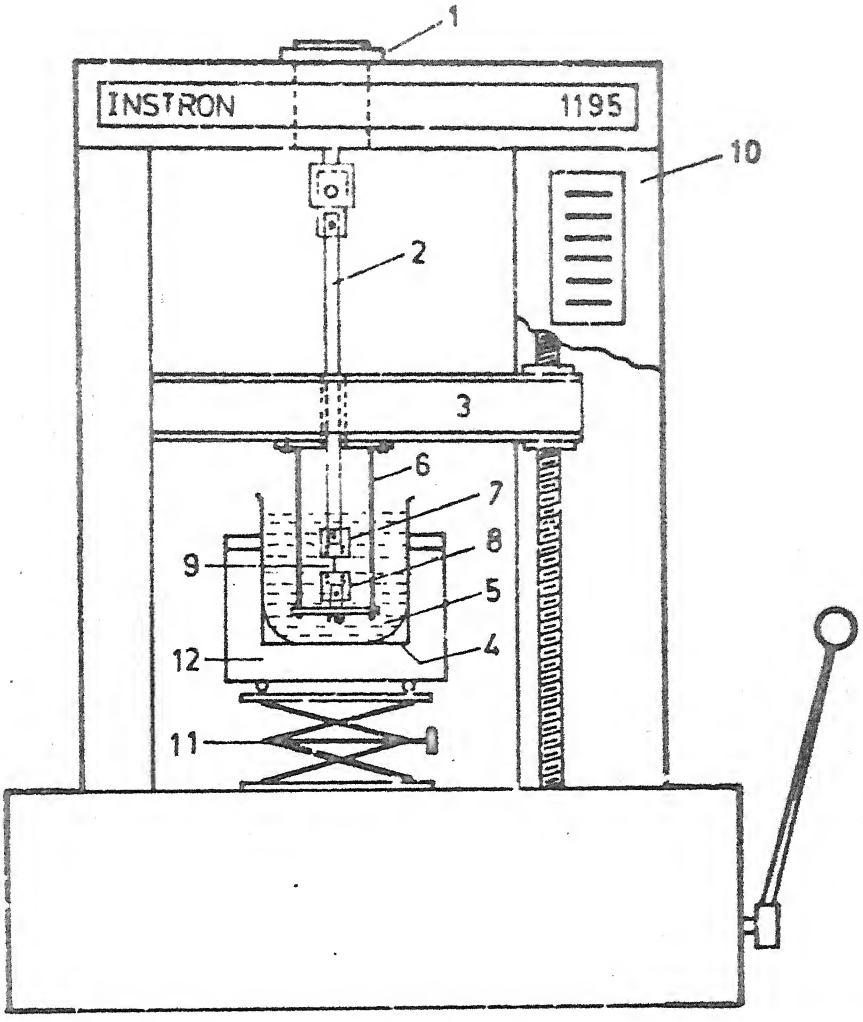

Fig. III.1 Schematic diagram of tensile stress relaxation fixture
(1) Load cell (2) M.S. bar (3) Cross head
(4) Oil bath (5) Silicon fluid (6) A cage containing the bottom grip and is held by four rods connected between lower and upper disc (7) Top grip
(8) Bottom grip (9) Specimen ; mettalic glass ribbon
(10) Instron universal testing machine (11) Jack
(12) Heating mantle.

This sample was then mounted between the two grips. Care was taken to ensure that the ribbon always remained vertical. After the temperature of the oil bath remained steady for a minimum of 60 minutes at the test temperature (453°K), the oil bath was raised over the sample. It took 45 seconds to raise the oil bath over the entire specimen length. In order to counteract the effect of thermal expansion of the grips and the surrounding rods, a small stress of the order of 5 - 15 MPa was applied. It was observed that there was a decrease in temperature due to raising of the oil bath. A preanneal of 30 min. was given in which the temperature stablized. Then the specimen was elastically loaded to the desired initial stress level. The motor of the machine was switched off and the load verses time plot was recorded. Once the experiment was over, the oil bath was lowered and samples were removed from the grips and preserved for further analysis.

III.4 Experimental Problems.

Considerable time was spent in solving the problems came up during the initial stages. In early experiments, approximately fifty minutes after loading, stress was found to increase slowly with time. This was more pronounced in some cases than in others. These plots are shown in figure III.2. It was earlier thought that this peculair behaviour may be due to the temperature instability. So the bath was heated up very much ahead of the test and was maintained at the test

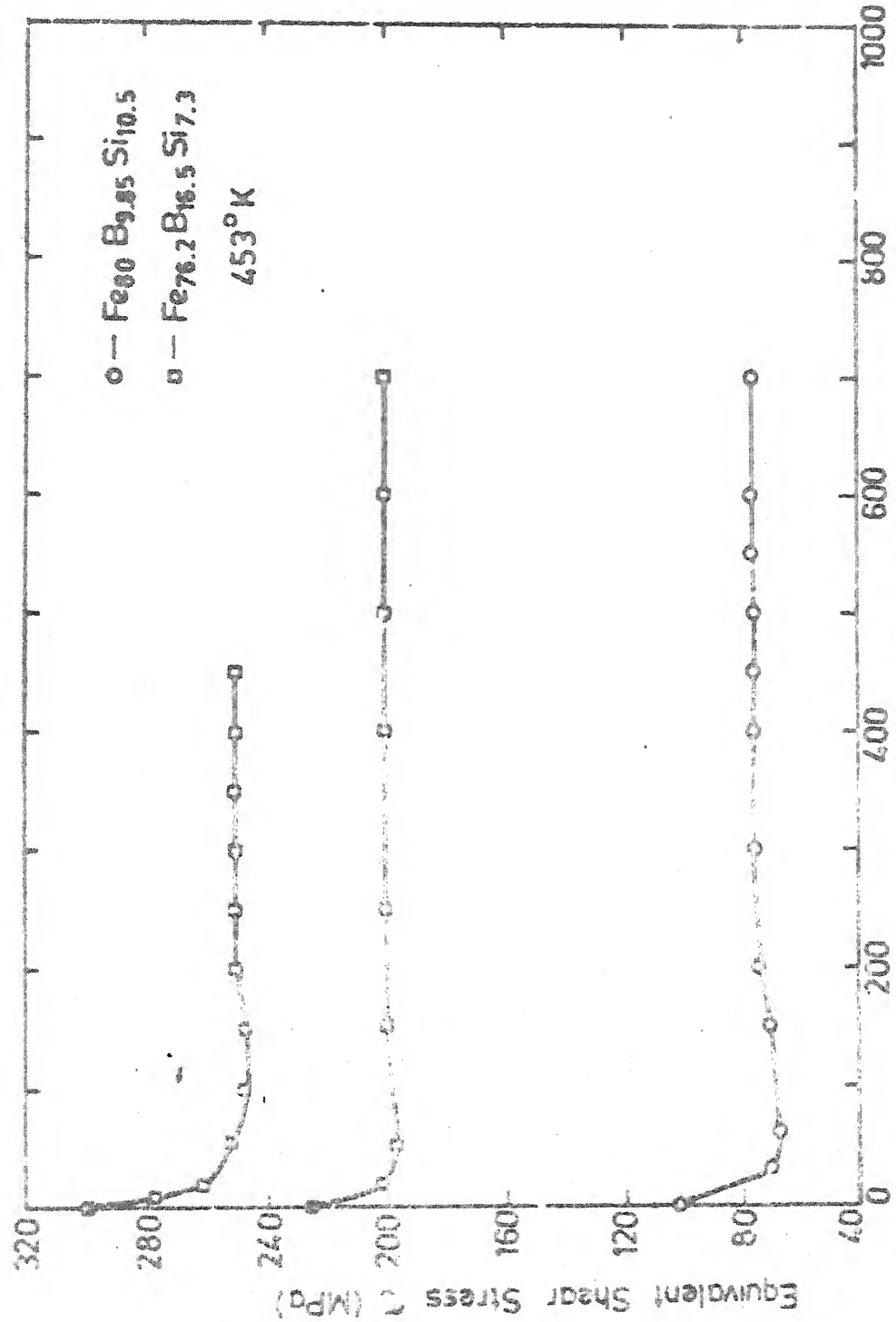

Fig. III.2 Equivalent shear stress as a function of time for as-cast samples tensile stress relaxation tested at 453°K starting at different initial stresses. The composition used are: $Fe_{80}B_{9.85}Si_{10.15}$ and $Fe_{76.2}B_{16.5}Si_{7.3}$. Note that the equivalent shear stress increases with time after t = 50 min.

temperature for a minimum of 200 min. However, this did not cure the problem.

When these samples were analysed by differential scanning calorimetery, it was found that the increase in stress may be due to the oxidation of the specimen. So in order to avoid oxidation, Argon gas, deoxidized by passing over heated copper turnings, was blown over the surface of the oil bath and also inside the oil bath. Also the top surface of the oil bath was covered by aluminium plates, suitably cut so as to accomodate the mild steel bar from the load cell and the four mild steel rods connected between the bottom plate and the cross head. These plates could be tightly placed and the gap between the plates was sealed using cotton wool and high temperature grease. After this modification, the problem of increase in stress with time was solved and good tensile stress relaxation like shown in fig. IV.1, IV.2

III.5 Bend stress relaxation experiment.

Bend stress relaxation experiment was carried out in an argon gas atmosphere. Three pyrex or aluminium rings of different radii were chosen. The ribbons were contrained into a ring so that the radius of curvature of the specimen were equal to the inner radius of the ring. These rings were kept in a pyrex tube of 38mm OD and 750mm long. A cylinder of copper sheet filled with copper turnings was kept in between the argon gas tube and the rings so that the deoxidized argon gas was once again made to pass through this heated

copper turnings. The pyrex tube was closed with a rubber cork having a hole for the argon gas tube to pass through.

This pyrex tube was evacuated and flushed with deoxidized argon gas for a minimum of three successive cycles. Then a positive pressure of argon gas was maintained through out the experiment. This pyrex tube was heated by a tube furnace whose temperature was maintained within $\pm 1^{\circ}C$. After annealing, the tube was taken out from the furnace and argon gas flow was allowed to continue till the tube was cooled.

III.6 Differential scanning calorimetry.

DSC studies were carried out using Dupont 910 differential scanning calorimeter. The specimen were cut into 2-3 mm length pieces. They were cleaned first in Trichloro-ethylene, then with acetone and finally with methanol. An empty aluminium pan was used as the reference. Experiments were carried out in a deoxidized argon gas atmosphere. The DSC cell was evacuated and flushed with deoxidized argon gas for three successive cycles and a weak argon gas pressure was maintained throughout the experiment. A heating rate of $20^{\circ}K/min.$ was used for all the runs . The set temperature, heating rate and other parameters were earlier programmed in a Dupont series 99 thermal analyser. The analysis of this data is discussed in chapter IV.

CHAPTER - IV

RESULTS AND DISCUSSIONS

IV.1. Tensile stress relaxation experiments.

These experiments were carried out at 453°K for two compositions namely $Fe_{80.2}\ B_{14.9}\ Si_{4.9}$ (composition I) and $Fe_{80.3}\ B_{12.4}\ Si_{7.3}$ (composition II). In composition I, stress relaxation tests were performed at five different initial stresses ranging from 70-400 MPa. For composition II, six different initial stress values between 115-700 MPa were used. Equivalent shear stress against time is plotted in figures IV.1 and IV.2 for the compositions I and II respectively Good reproduciability was found when these experiments were repeated with the same value of initial stress and the plots in Figs. IV.1 and IV.2 are the averages of upto three runs, the size of the points indicating the amount of scatter. Youngs modulus E was calculated from the slope of the linear region during loading. Width, thickness and Young's modulus values of the ribbons are tabulated in table IV.1.

IV.1.1 Analysis of the stress relaxation data.

Load-time plots are converted into tensile stress-strain plots using the relation

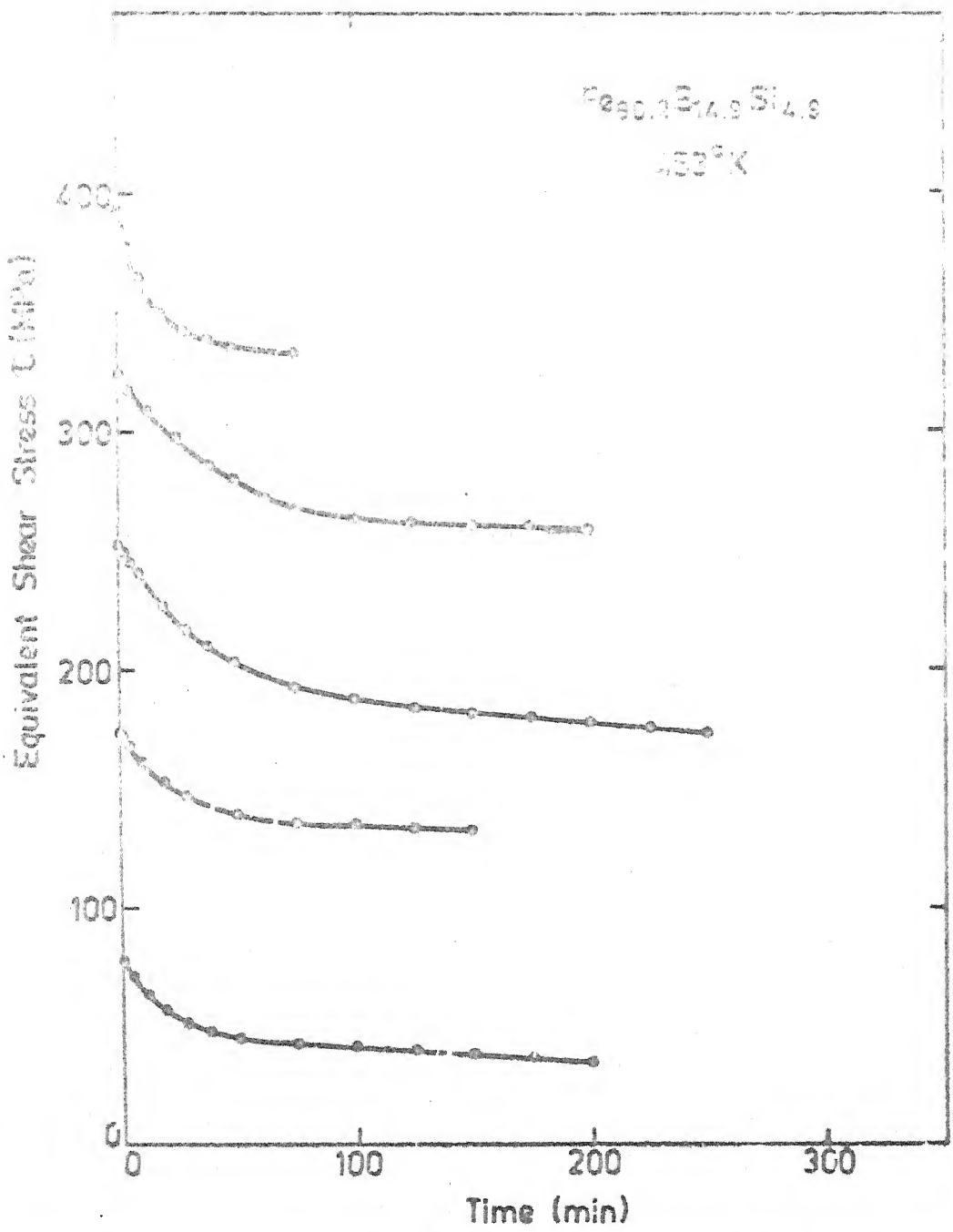

Fig. IV.1 Equivalent shear stress as a function of time for as cast $Fe_{80.2}B_{14.9}Si_{4.9}$ samples tensile stress relaxation tested at 453°K starting at different initial stresses.

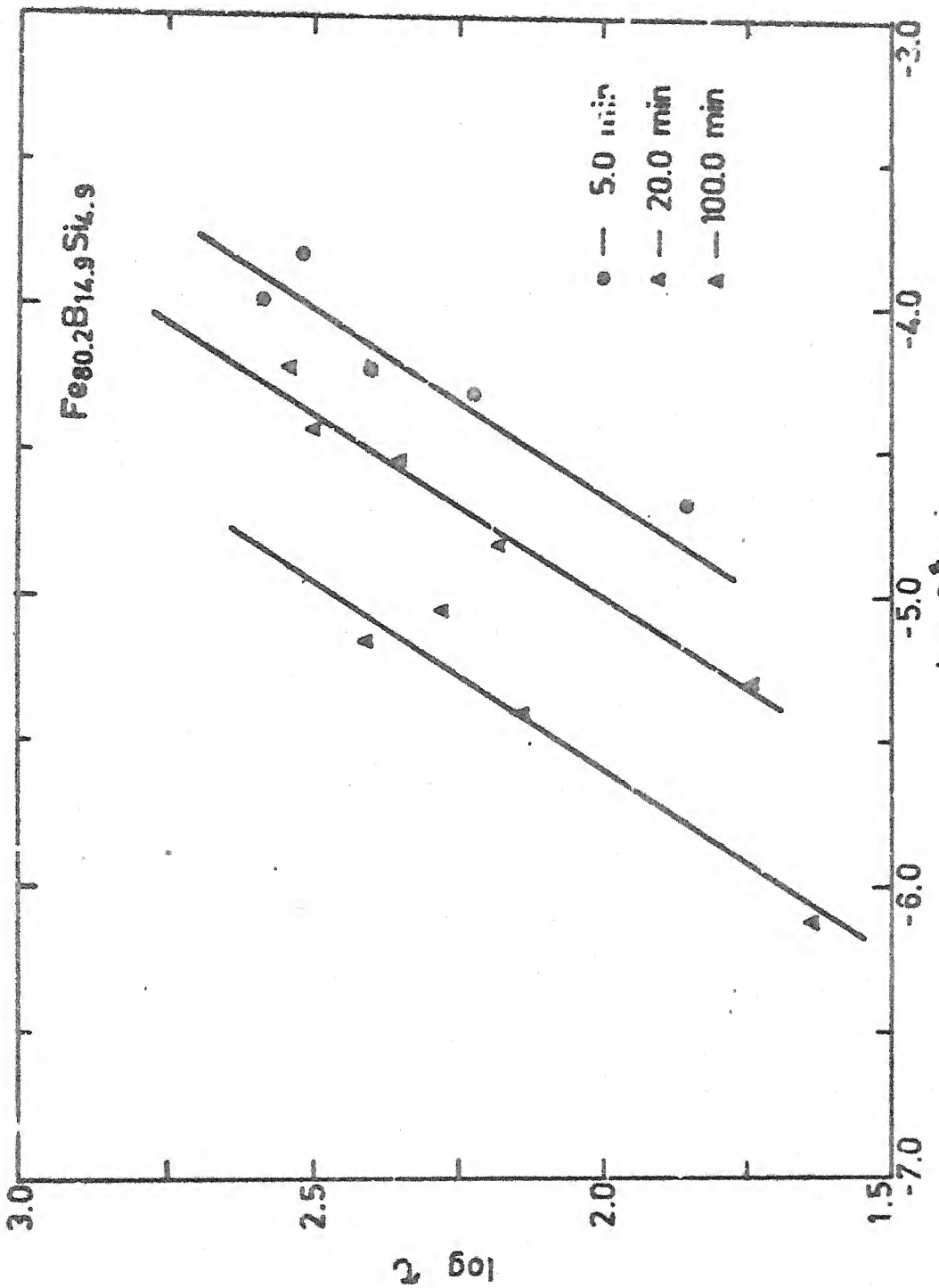

Fig. IV.2 Shear strain rates at indicated times of tensile stress relaxation curves in fig. IV.1 cross plotted with equivalent shear stress. Solid line indicates the

TABLE IV. 1

Width, Thickness and Youngs' modulus data for Compositions I II III

Composition	Width mm	Thickness mm	Youngs' modulus GPa
$Fe_{80.2}B_{14.9}Si_{4.9}$ (Composition I)	1.114 ± 0.010	0.029 ± 0.002	115.1 ± 12.0
$Fe_{80.3}B_{12.4}Si_{7.3}$ (Composition II)	0.808 ± 0.004	0.015 ± 0.001	110.1 ± 10.2
$Fe_{75.8}B_{17.4}Si_{6.8}$ (Composition III)	0.604 ± 0.005	0.024 ± 0.003	126.6 ± 8.7

$$\text{Tensile stress } \sigma = \frac{\text{Load (Kg)} \times 9.806}{\text{width(mm)} \times \text{Thickness (mm)}} \text{ MPa} \quad \ldots \text{IV.1}$$

$$\left[1\text{Mpa} = 10^6 \frac{\text{N}}{\text{m}^2} \right]$$

This tensile stress is further converted into equivalent shear stress according to the relation, equivalent shear stress $\tau = \frac{\sigma}{\sqrt{3}}$. Assuming that the machine is infinitely stiff,

$$\frac{d\sigma}{dt} = -E\dot{\epsilon} \quad \ldots\ldots \text{IV.2.}$$

$$\frac{d\tau}{dt} = \frac{1}{\sqrt{3}} \frac{d\sigma}{dt} = -\frac{1}{\sqrt{3}} E. \frac{\dot{\gamma}}{\sqrt{3}} = \frac{-E\dot{\gamma}}{\sqrt{3}\cdot\sqrt{3}}$$

Since $\dot{\gamma} = \sqrt{3}\dot{\epsilon}$ [62]. Therefore the shear strain rate is given by

$$\dot{\gamma} = \frac{-3}{E} \frac{d\tau}{dt} \quad \ldots\ldots \text{IV.3}$$

where $\frac{d\tau}{dt}$ is slope of the $\tau - \dot{\gamma}$ plot at any time t. The values of $\dot{\gamma}$ is plotted against the corresponding values of τ at a time t. The slope of the $\log \dot{\gamma}$ -$\log \tau$ curve gives the value of strains rate sensitivity index m which is stated as

$$m = \frac{\partial \log \dot{\gamma}}{\partial \log \tau} \quad \ldots\ldots\ldots \text{IV.4.}$$

Viscosity of the metallic glass ribbons is calculated from

$$\eta = \frac{\tau}{\dot{\gamma}} \quad \text{IV.5}$$

and rate of change of viscosity with time is calculated from the slope of the viscosity time plot.

IV.1.2 Results.

IV.1.2.1 Composition I.

The equivalent shear stress τ as a function of time t for the as cast samples of composition I ($Fe_{80.2}B_{14.9}Si_{4.9}$) is shown in Fig. IV.1. In Fig. IV.2. equivalent shear strain rate is plotted against equivalent shear stress. The scattering of data points in this plot may be attributed to same non-uniformity of the ribbons and may be due to the irregular cross-sections that exist in the ribbons dispite polishing the edges. Since the maximum initial equivalent shear stress used in the experiment is approximately equal to 400 MPa, linear shear strain rate - shear stress behaviour i.e. Newtonian viscous flow may be expected. Hence, the least square straight line fit was employed and is shown in Fig. IV.2 (Solid line). The strain rate sensitivity index m, which is the slope to

the curve, was found out to be between 1.2 and 1.5. By applying transition state theory to the flow processes, an equation describing the shear strain rate variation with the variation of equivalent shear stress is given as follows

$$\dot{\gamma} = \dot{\gamma}_o \sinh \frac{\tau \gamma_o \Omega_f}{kT} \quad \ldots\ldots \text{IV.6 [37]}$$

Then the strain rate sensitivity index m is given by

$$m = \frac{d \log \dot{\gamma}}{d \log \epsilon} = \frac{\tau \gamma_o \Omega_f}{kT} \coth \frac{\tau \gamma_o \Omega_f}{kT} \quad \ldots\ldots \text{IV.7}$$

$\coth \left(\frac{\tau \gamma_o \Omega_f}{kT} \right) = \frac{\tau \gamma_o \Omega_f}{kT}$ for small values of $\frac{\tau \gamma_c \Omega_f}{kT}$ [50]

Then m is given by $m = \left(\frac{\tau \gamma_o \Omega_f}{kT} \right)^2$ or

$$\gamma_o \Omega_f = \frac{\sqrt{m}\, kT}{\tau} \quad \ldots\ldots\ldots \text{IV.8}$$

Thus calculated values of $\gamma_o \Omega_f$ are used in the equation IV.6 for the calculation of $\dot{\gamma}$. Thus calculated values of nearly overlap over the least swuare straight line fit.

We have tried to fit our data to the equation IV.6 using iteration process. The details of the process are given in appendix I. With this program a well defined minimum for the least square error could not be obtained. Fluctuations in the minimum value of this least square error was found and hence further analysis could not be done.

The effective increase in viscosity is plotted against time in Fig.IV.3 and is found to increase linearly with time. In the initial period of the relaxation tests, due to atomic rearrangements, motion of the defects, the viscosity of the ribbons should be less. As time increases, these movements slowly cease, thus resulting in an increase in viscosity. The rate of change of viscosity is calculated from the slope of this curve.

IV.1.2.2 Composition II.

The equivalent shear stress as a function of time is shown in figure IV.4. The corresponding equivalent shear strain rate is plotted as a function of equivalent shear stress in in figure IV.5. It is found that the shear strain-rate values deviate from a linear increase with equivalent shear for shear stresses $\gtrsim$ 500 MPa.

Similar behaviour have been observed by Taub and Luborsky [51] Since these data could not be fitted to the flow equation derived from transition state theory, i.e.

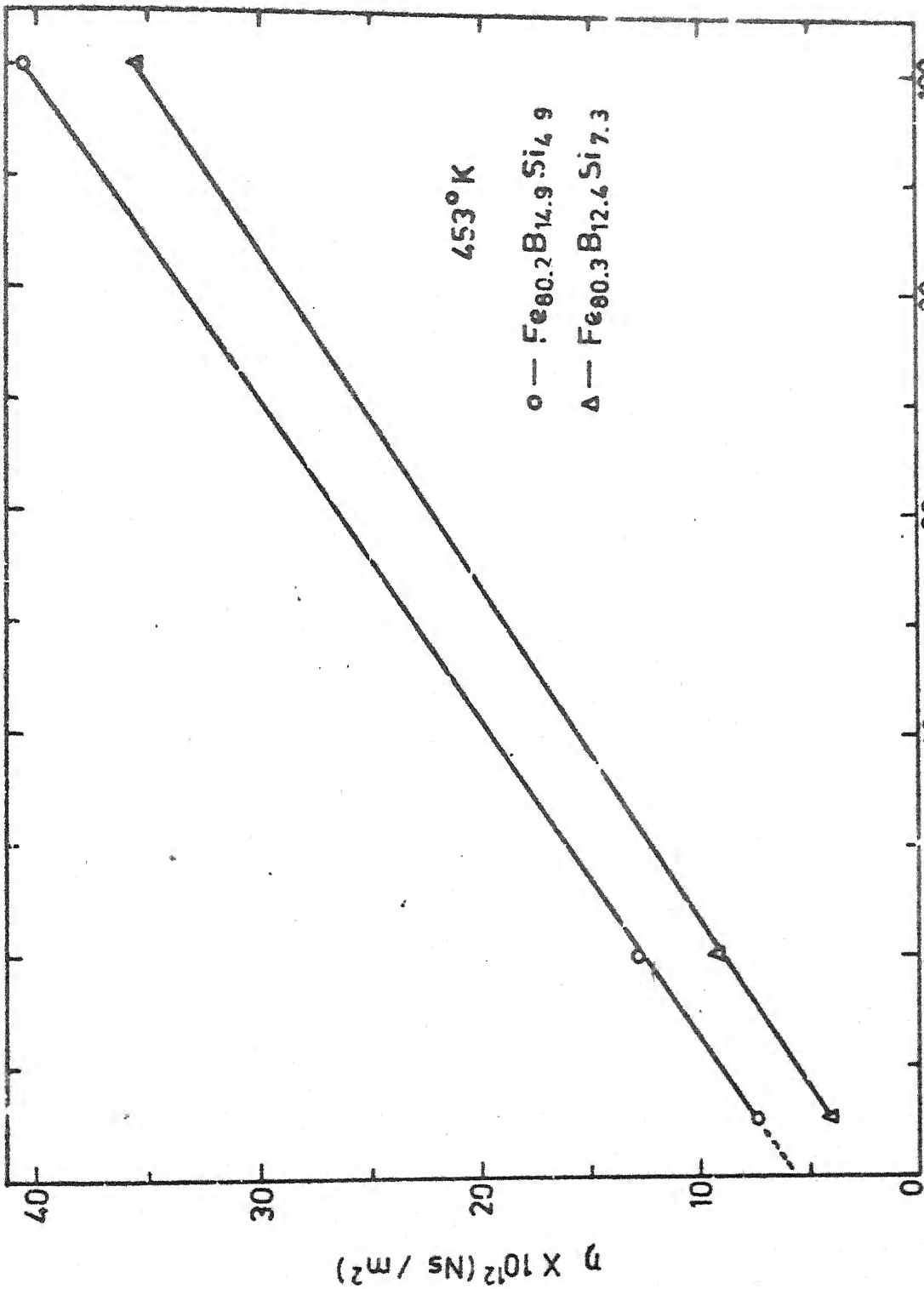

Fig. IV.3 Effective viscosity increase computed from tensile stress relaxation data in fig. IV.1 and IV.4 for the compositions indicated.

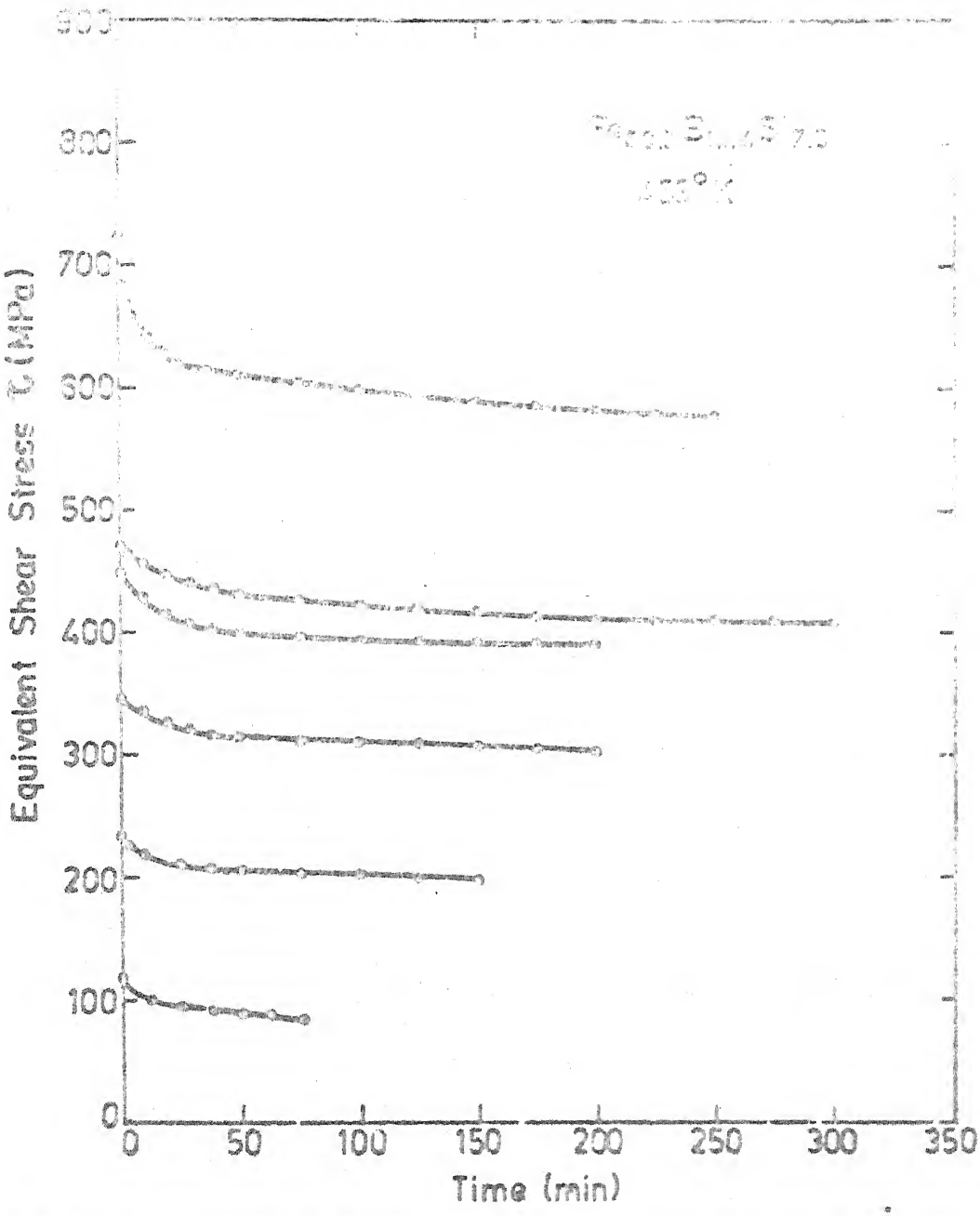

Fig. IV.4 Equivalent shear stress as a function of time for as cast $Fe_{80.3}B_{12.4}Si_{7.3}$ samples tensile stress relaxation tested at 453°K starting at different initial stresses.

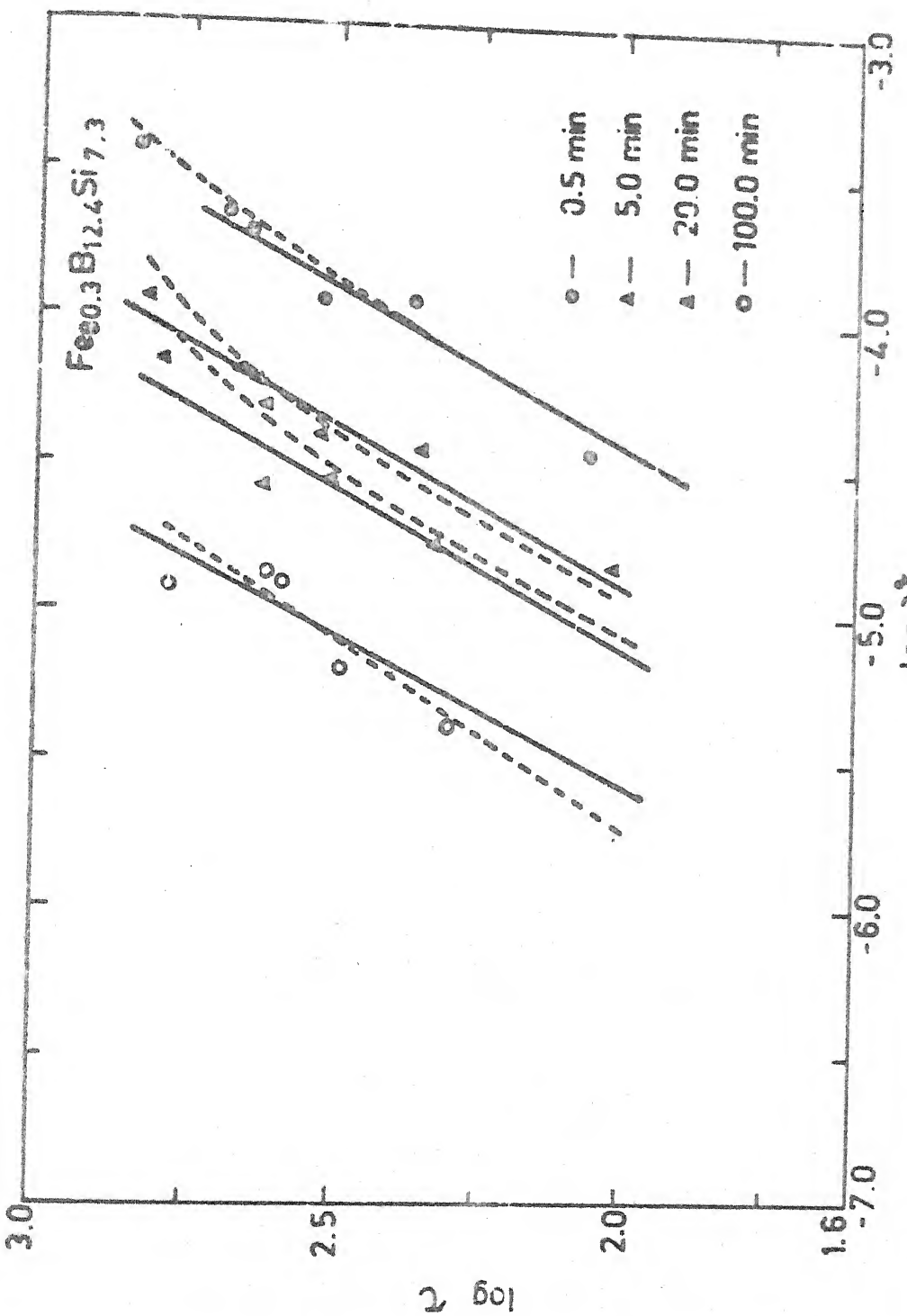

Fig. IV.5 Shear strain rates at indicated times of tensile stress relaxation curves in fig. IV.4 cross plotted with equivalent shear stress. Solid lines indicte the least square fit for the linear portion. Dotted lines indicate the least square fit with atomic volume element, calculated from the slope of the linear region.

equation 6, an alternative approach as described in the earlier section has been used and thus calculated shear strain rates are shown in figure IV.5 as dotted lines. The fit is quite good. The strain rate sensitivity index calculated from the Fig. IV.5 vary from 1.06 to 1.133 for the linear region and 1.85 to 2.75 in the non-linear region. The data used in equation (6) fitting are shown in table IV.2

A linear increase in viscosity with time has been observed and is shown in Fig. IV.3. At a particular time, viscosity for composition II lines above for composition I. The rate of change of viscosities are computed from the slope of the figure IB.3.

IV.2. Bend Stress Relaxation Experiments.

Besides the two compositions mentioned earlier, bend stress relaxation experiments were also carried out for another composition $Fe_{75.8}\ B_{17.4}\ Si_{6.8}$ (composition III). This experiment was carried out for six different temperatures and at each temperature for form different times except for composition III where only five temperatures were used. The actual experimental conditions are shown in table IV.3.

Two pyrex rings of inner radii 8.05, 6.75 mm and one aluminium ring of 6.75 mm dia were chosen. The ribbons were constrained inside a ring and annealed at desired temperature. Then to samples were taken out of the ring and their final radii

TABLE IV.2

Data showing the parameters used in fitting to Equation IV.6 to the experimental set of data points.

Time → / Composition ↓		0.5 Min.	5 Min.	20 min.	100 min.
$Fe_{80.2}B_{14.9}Si_{4.9}$	m		1.275	1.45	1.28
	$\gamma_o \Omega_f$ Å^3		28.09	32.265	38.61
	γ_o x10^{-6} s^{-1}		56.509	17.923	3.86027
$Fe_{80.3}B_{12.4}Si_{7.3}$					
Linear region	m	1.081	1.103	1.081	1.0667
Non-Linear portion.	m	2.75	2.70	1.85	
	$\gamma_o \Omega_f$ Å^3	18.06	21.44	20.19	19.706
	γ_o x 10^{-6} s^{-1}	112.49	29.474	25.99	6.7237

TABLE IV.3

Experimental Conditions during bend stress relaxation tests.

Temperature °K	423	453	483	513	543	573
Time (min)	20, 100, 500, 1000	20, 100, 630 1000	20, 100 500, 1000	20, 100, 500, 1000	20, 100, 500, 860	20, 100, 500, 1000
Composition	I, II	I, II, III	I, II, III	I, II, III	I, II III	I, II III

of curvature were measured. The procedure for analysis of the data is given below.

IV.2.1. Analysis of the bend stress relaxation data.

Let γ_i and γ_f are the radii of curvatures of the r ribbons when kept in a ring before annealing and after the experiment, respectively. The maximum bending stress during initial stages is given by [63]

$$\sigma_o = \frac{Et}{2\gamma_i} \quad \rightarrow \quad \text{IV.9}$$

The maximum bending stress relieved is given by

$$\sigma = \frac{Et}{2\gamma_i} - \frac{Et}{2\gamma_f} = \frac{Et}{2}\left(\frac{\gamma_f - \gamma_i}{\gamma_i \gamma_f}\right)$$

Stress relaxation ratio

$$= \sigma/\sigma_o = \frac{\gamma_f - \gamma_i}{\gamma_f} \quad \ldots\ldots \text{IV.10}$$

Also the equivalent shear strain rate is given by

$$\dot{\gamma} \frac{d\gamma}{dt} = -\frac{3}{E} \frac{d\tau}{dt} \quad \ldots\ldots \text{IV.3}$$

For Newtonian viscosity $\tau = \eta\dot{\gamma}$ Substitutes this in equation IV.3, For low stresses,

$$\frac{d\tau}{dt} = \frac{-E}{3} \quad \frac{\tau}{\eta} = \frac{-E}{3} \frac{\tau}{\dot{\eta} t + \eta_o} \qquad \text{IV.11}$$

[In this study the maximum bending shear stress during bend stress relaxation is 200 MPa and η_o is to initial viscosity.

Integrating from t = 0 with initial stress = τ_o

we get

$$\ln \frac{\tau}{\tau_o} = \frac{-E}{3\dot{\eta}'} \ln t.$$

So after an initial transient, $\ln \frac{\tau}{\tau_o} = \ln \sigma/\sigma_o$ should decrease linearly with lnt. With the slope equal to $-E/3\dot{\eta}$

IV.2.2. Results.

The logarethmic bend stress relaxation ratio σ/σ_o is plotted against log t. For the compositions I, II, and III in figures IV.6, IV.7 and IV.8 respectively. After an initial transient, log σ/σ_o isfound to decrease linearly with log t. From the slope of the linear (Slope = $\frac{-E}{3\dot{\eta}}$) portion the rate of change of viscosity $\dot{\eta}'$ can be calculated using the values of the Youngs modulus E. This rate of change of viscosity is plotted against temperature in Fig. IV.9. It is seem that rate of viscosity change is high for the ribbons where the stress relaxation is less. If the initial and final viscosities of these ribbons are nearly the same, then

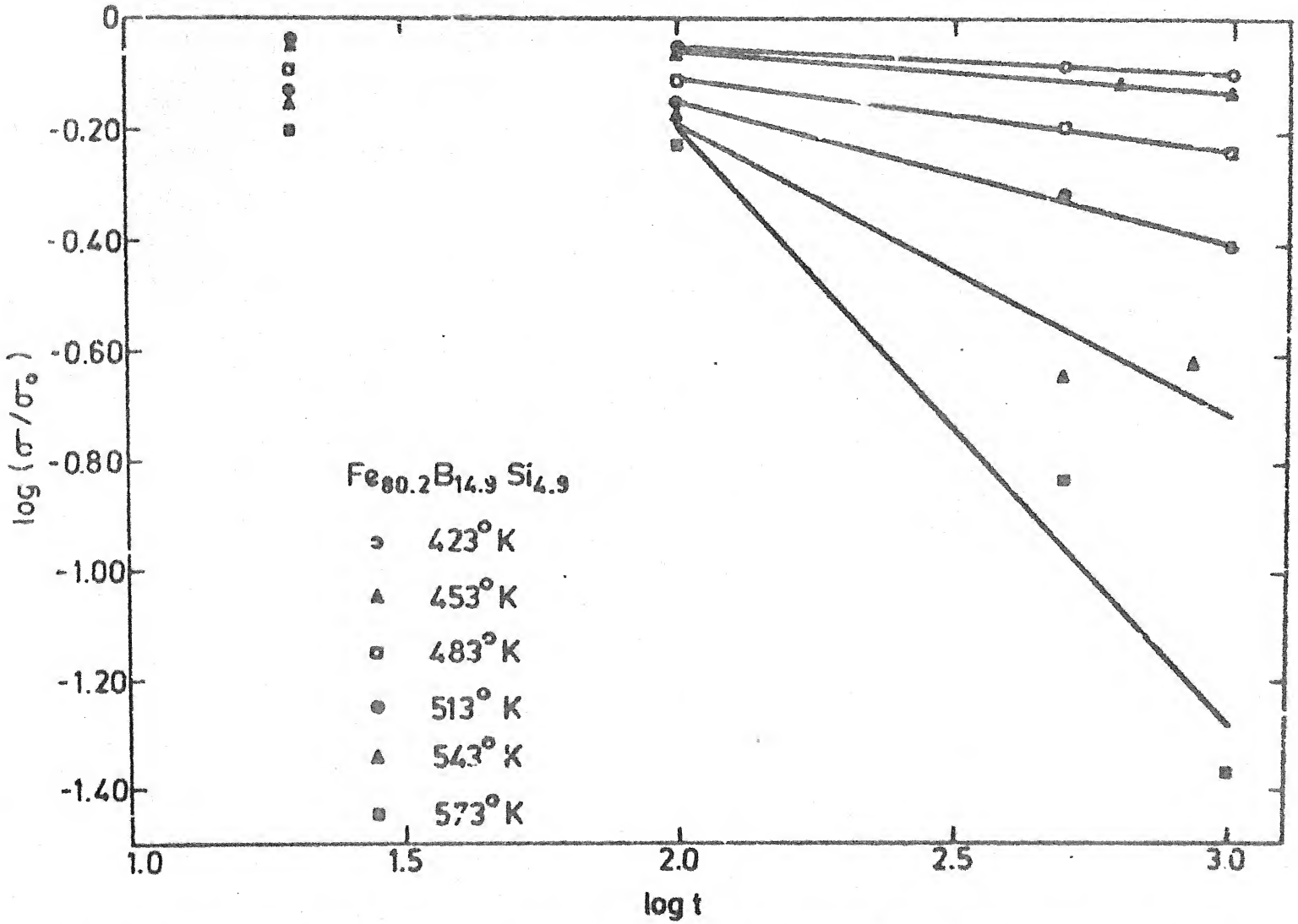

Fig. IV.6 Bend stress relaxation data for as cast $Fe_{80.2}B_{14.9}Si_{4.9}$ ribbons at the indicated temperatures. The solid lines indicate the slope of the linear region.

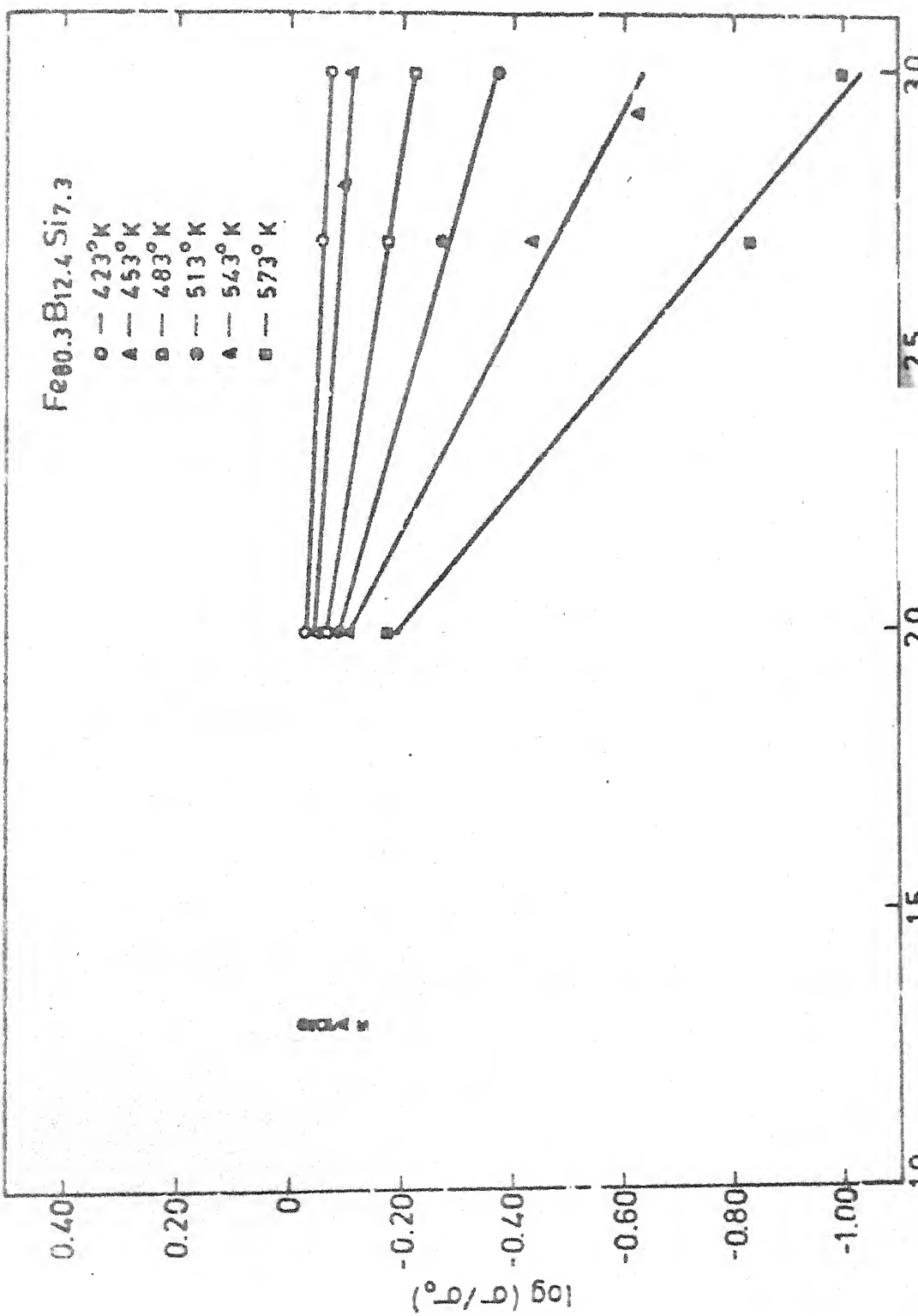

Fig. IV.7 Bend stress relaxation data for as cast $Fe_{80.3}B_{12.4}Si_{7.3}$ ribbons at the indicated temperatures. The solid lines indicate the slope of the linear region.

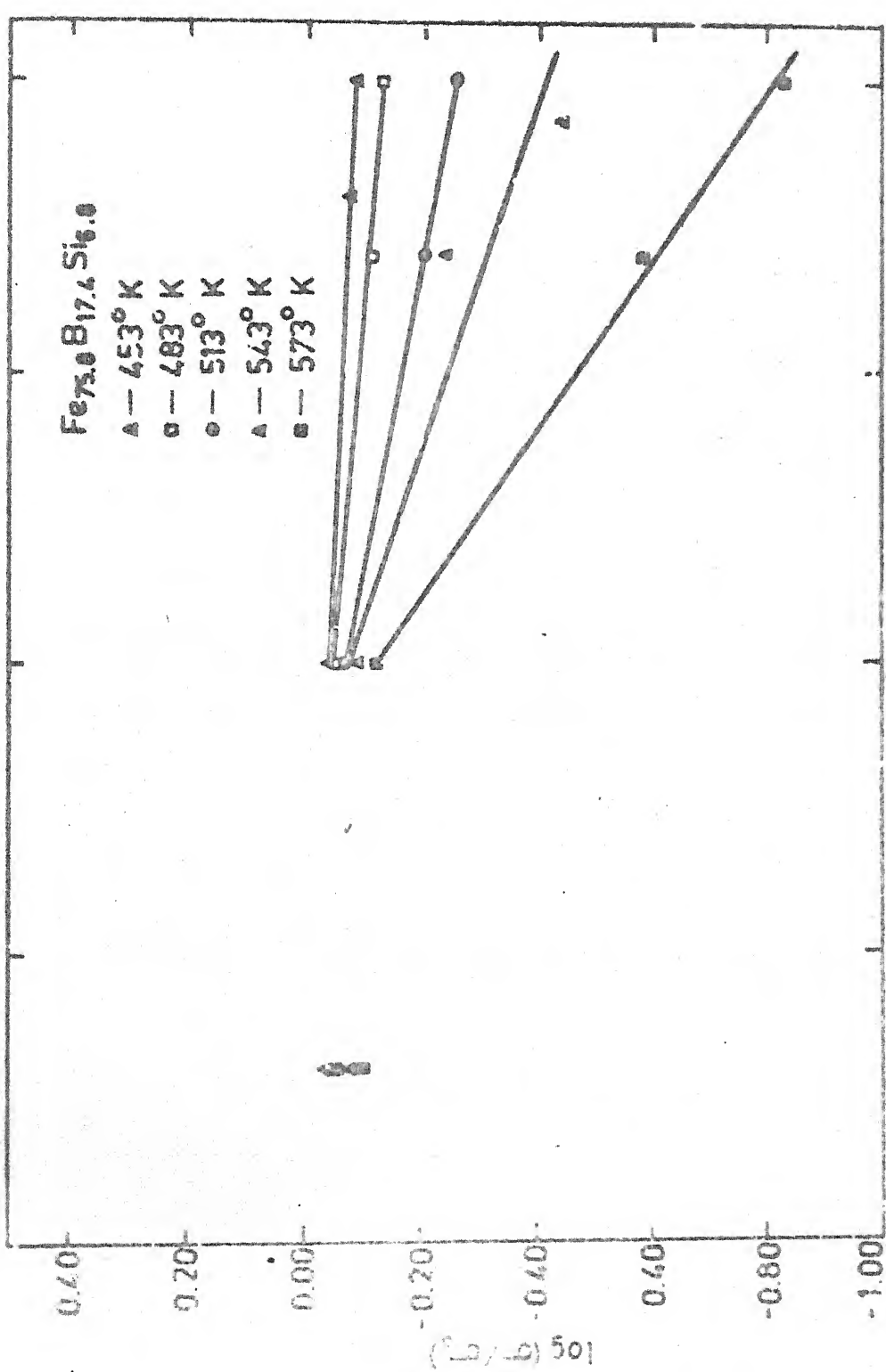

Fig. IV.8 Bend-stress relaxation data for as cast $Fe_{75.8}B_{17.4}Si_{6.8}$ ribbons at the indicated temperatures. The solid lines indicate the slope of the linear region

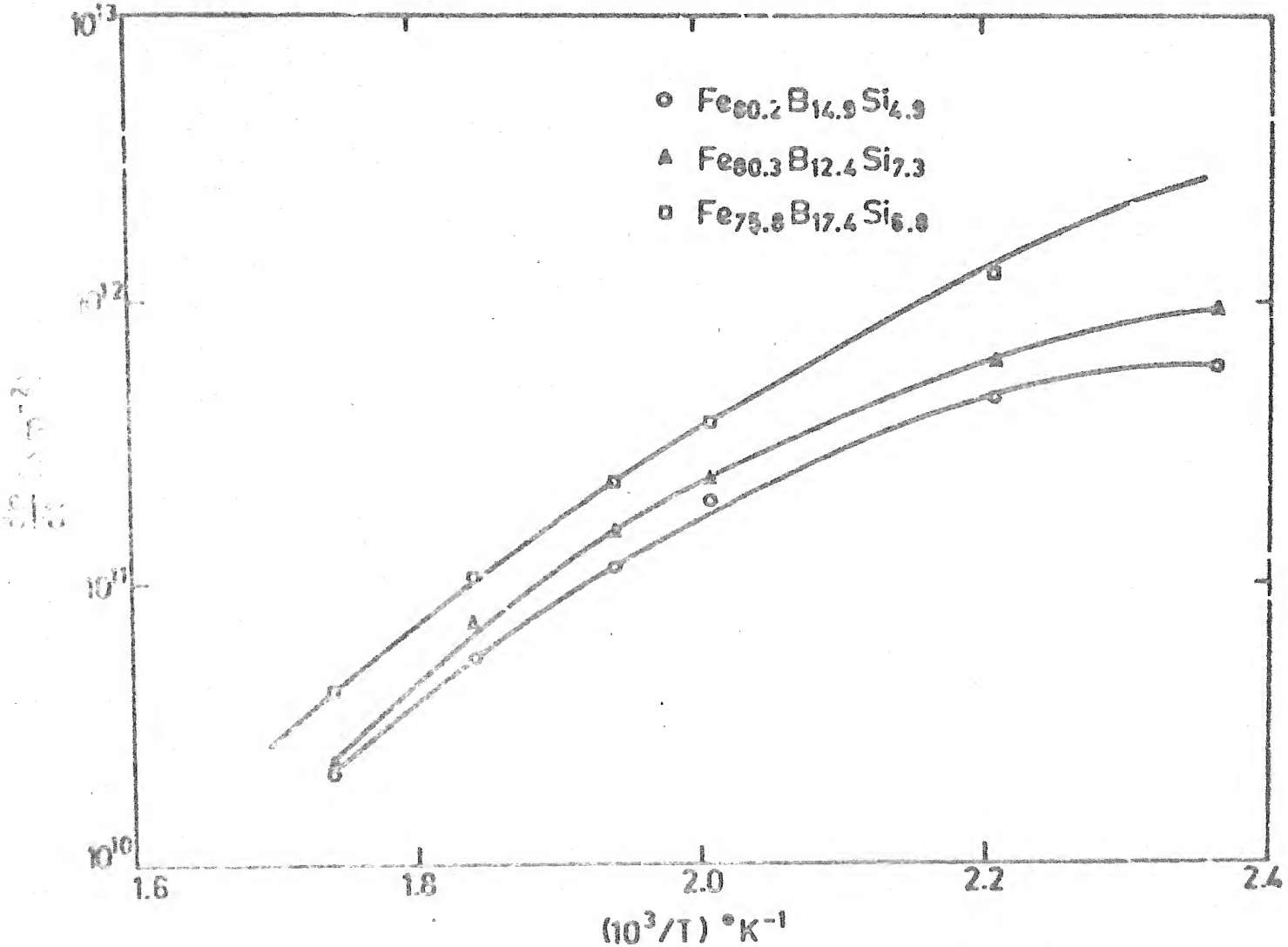

Fig. IV.9 Rate of change of viscosity with time as measured in 2and stress relaxation tests for the compositions indicated in the figure.

in the compssition III, where the amount of stress relaxation is the least, to stable glass configuration is attained qhickly this explaining the higher values of $\dot{\eta}$. For the composition I, where the bend stress relaxation is more the glass may have to pass through several metastable states before reaching to stable glassy state and hence the rate of viscosity change may be less. When these values are compared with the rate of change of viscosity obtained from tensile stress relaxation data, it was observed that the rate of change of viscosity for tensile stress relaxation values are slightly lower than the rate of viscosity change for bend stress relaxation. Since the rate of change of viscosity is independent of annealing, it can not be explained by pre-annealing the ribbons for 30 min. during tensile stress relaxation experiments. Probably this may be due to scattering of experimental data points.

Walter and Luborsky [63] have suggested an emperical relation regardingthe effectivness of various elements in contributing to the stress relaxation. This effectiveness in increasing order as follows.

Al, Si $<$ B $<$ Fe $<$ Ni. our results tend to support this relation. Thus higher the boron content in our compositions I as compared to composition II leads to greater stress relaxation in composition I than in composition II.

Similarly decrease in the amount of iron in Composition III decreases relaxation to a large extent. Also the stress relaxation is less for Fe B Si ribbons then for Fe Ni PB ribbons, which may be because the presence of Ni in the latter.

IV.3 Differential Scanning Calorimeter.

Experiments were carried out in a Dopant 910 differential scanning calorimeter. The samples were heated up from 323°K to 800°K and the differences in heat in put - temperature plot was obtained. A calibration run on sapphire where specific heat is known, was made under similar conditions. The heating rate used was 20°K/min. A run with empty pan was made for calculation of the specific heat under the similar conditions. If ΔY is the distance of the curve for empty pan, from the base line at a particular temperature, $\Delta Y1$ and $\Delta Y2$ ar those for the sapphire and ribbon at the same temperature, then specific heat of the sample at htat temperature is given by

$$C_p = \frac{m_{SaP}}{m_{sample}} \times \frac{(\Delta Y2 + \Delta Y)}{(\Delta Y1 + \Delta Y)} \times C_p\, Al_2O_3$$

where

$C_p\, Al_2O_3$ is the specific heat of the sapphire at that temperature

m_{sap} and m_{sample} are the masses of the sapphire and ribbons respectively.

Thus calculated values of C_p were plotted against the corresponding temperature.

When a metallic glass ribbon is annealed at a high temperature, the atomic structure is driven from the state that was frozen in during the quenching into the direction of a metastable equilibrium releasing excess heat in the process. Hence, the specific heat of the as-cast ribbons should be above the specific heat of the annealed ribbons. This was observed when a sample was reseen in DSC itself after being first scanned to 623°K in argon atmosphere (Fig.IV.10). when the ribbons were annealed in copper boat in the argon atmosphere and subsequently analysed by differential scanning calorimetry, reverse bend was observed. Fig (IV.10, IV.11) when the samples subjected to a stress were annealed in the argon atmosphere , and analysed in DSC, strange behaviours were found. In one case, the specific heat curve lies above the as-cast specific heat curve (Fig. IV.11) whereas in the other case both the curves for the annealing with stress samples lie below that of the as-cast curve. (Fig. IV.12) The exact reasons for these annealing are not known, but can be due to sample oxidater or sample handling procedures. Because of the DSC data is not presented.

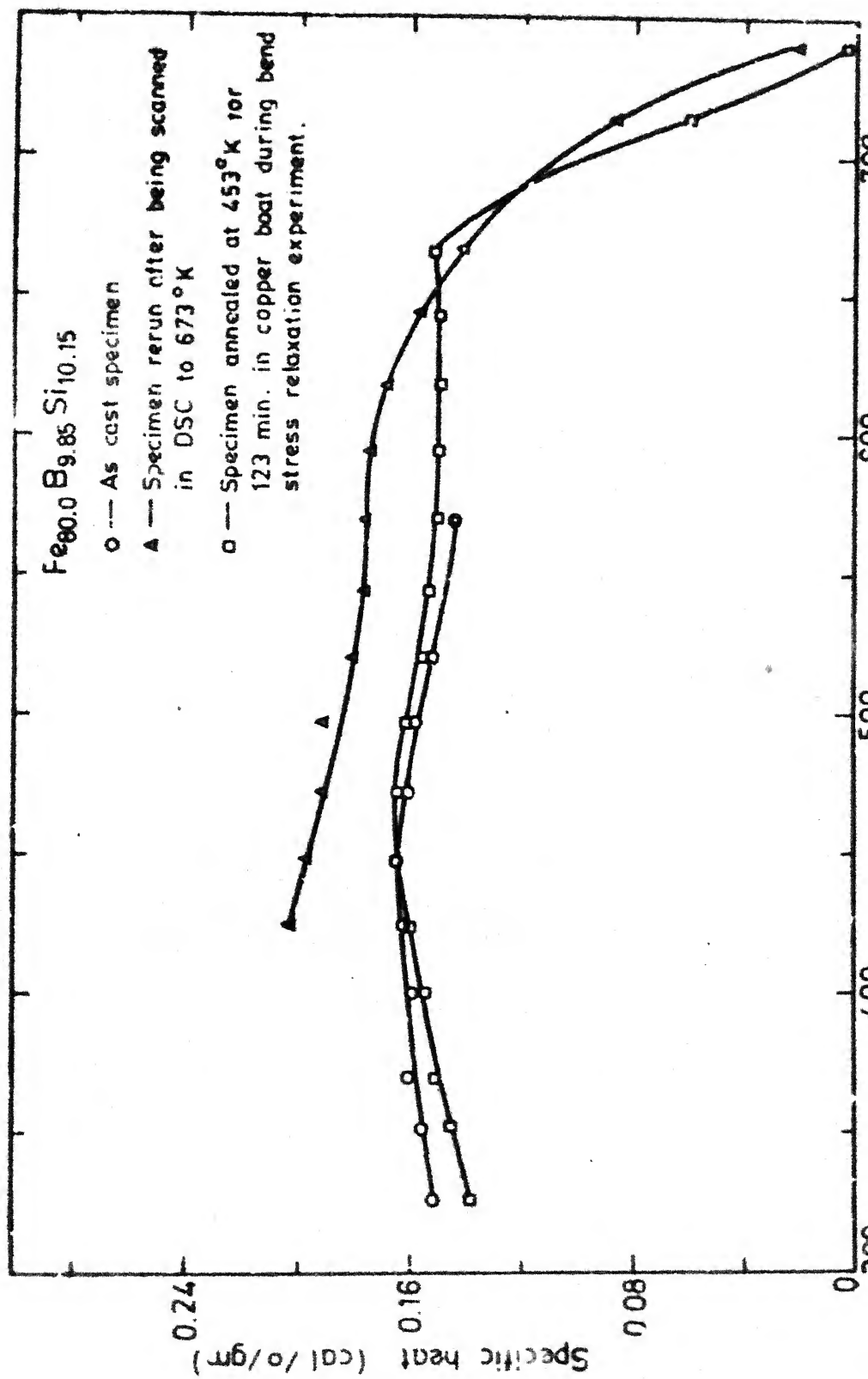

Fig. IV.10 Specific heat Vs temperature for as cast and annealed samples of $Fe_{80}B_{9.85}Si_{10.15}$ ribbon.

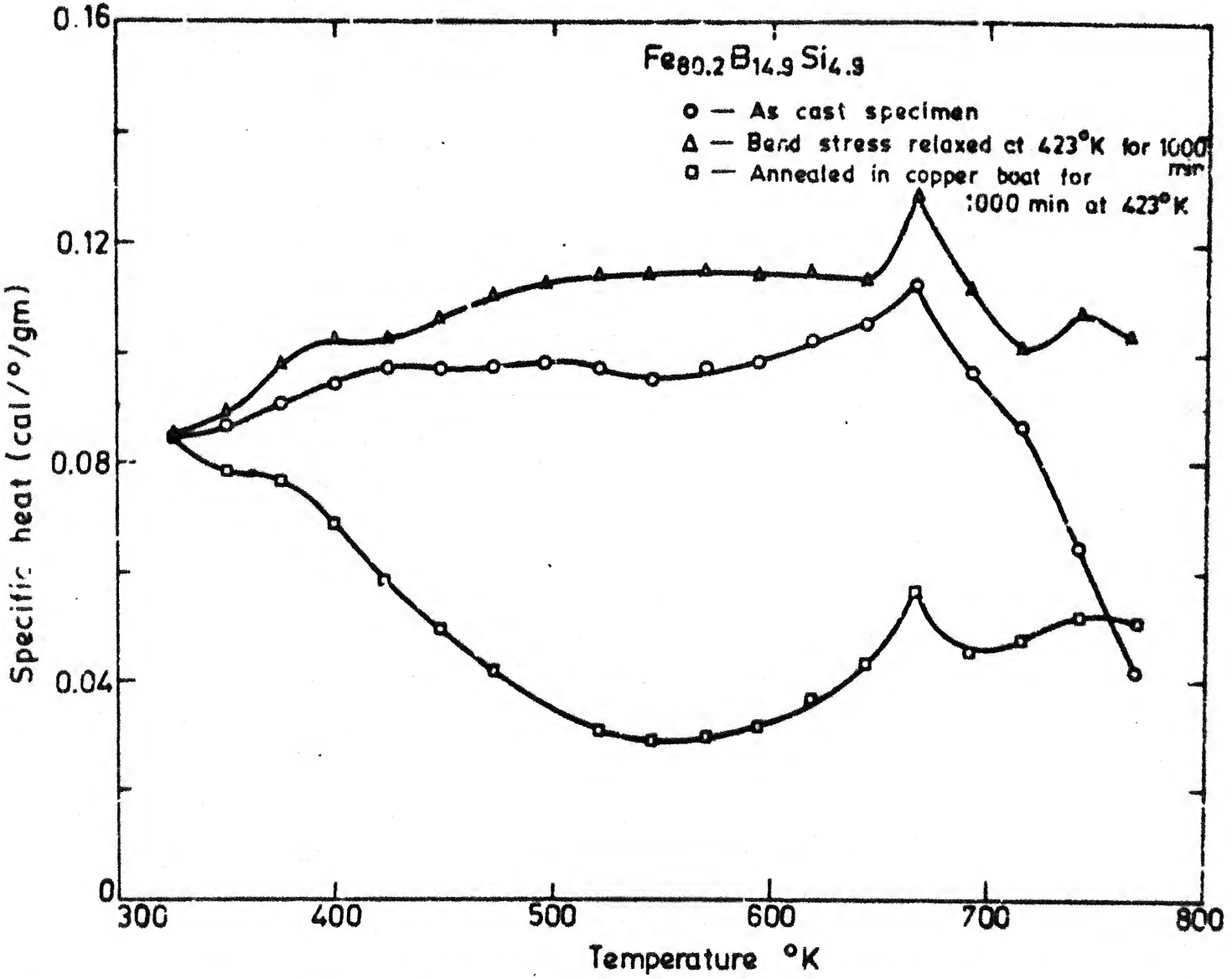

Fig. IV.11 Specific heat Vs temperature for as cast, anneled and bend stress relaxed samples of $Fe_{80.2}B_{14.9}Si_{4.9}$ ribbon.

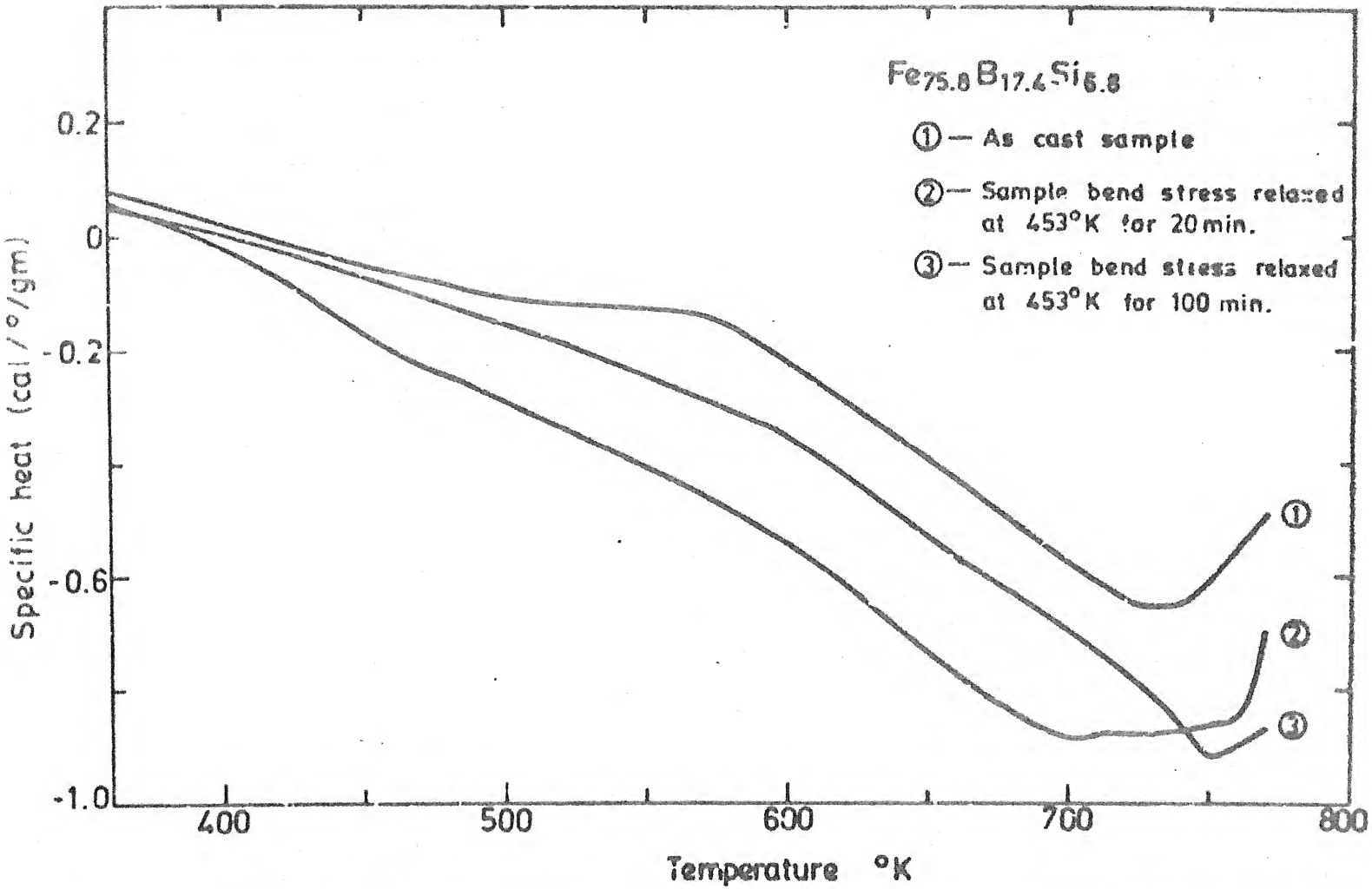

Fig. IV.12 Specific heat Vs temperature for as cast and bend stress relaxed samples of $Fe_{75.8}B_{17.4}Si_{6.8}$ ribbon.

CHAPTER - V

S U M M A R Y

Iron-Boron-Silicon system was chosen for the present study. This system is of technologically important because of its excellent magnetic and corrosion resistant properties. Stress relaxation behaviour is known to affect this properties because of the structural changes during relaxation. So the relaxation behaviour of these materials should be known inorder to increase their utility. So far very limited number of stress-relaxation experiments have been carried out using this composition. Hence, the present study was undertaken to get more knowledge about the relaxation behaviour of Fe-B-Si metallic glass ribbons.

Metallic glass ribbons were made using chill block melt spinning techniques. Stress relaxation behaviour was studied using Tensile, bend techniques. Stress relaxation experiments were carried out for three compositions in Fe-B-Si system which are in the amorphous range. An experimental arrangement used for tensile stress relaxation was designed. Earlier problems were overcome by modifying the experimental design and reproduciable stress relacation plots have been obtained. The data was analysed to yield strain rate sensitivity index, change of viscosity with time and rate of change of viscosity. Strain rate sensitivity index was found to vary from unity in the low stress region to 2.75 in

high stress region. A fit of the hyperbolic sine relation for the shear stress was attempted with the experimental values of strain rate but it was not possible because of the high values of error function. Linear increase in viscosity with time was observed. Rate of change of viscosity with time was calculated.

Bend stress relaxation experiments were performed for three compotions over a range of temperatures. After an initial transient, stress relaxation ratio was found to decrease with time. Rate of change of viscosity with time was calculated at different temperatures. Stress relaxation for the three compositions under the same conditions is given in the decreasing order

$$Fe_{80.2}\ B_{14.9}\ Si_{4.9} > Fe_{80.3}\ B_{12.4}\ Si_{7.3} >$$

$$Fe_{75.8}\ B_{17.4}\ Si_{6.8}$$

where as reverse trend was found in the rate of change of viscosity. In general stress relaxation behaviour of Fe-B-Si metallic glass ribbons agreed with the relaxation behaviour reported in the literature for other compositions.

REFERENCES

1. W. Klement,JR. , R.H. Willens and P. Duwez, Nature 187 (1960) 809.
2. S. Mader, J. Vac. Sci. Tech., 2 (1965) 35
3. D.B. Bagley and D.T. Turnbull, J. Appl. Phys., 34, (1968) 5681
4. H. Jones and C. Suryanarayana, J. Mater. Sci. 8, (1973) 705.
5. H. Jones, Rep. Prog. Phys., 36, (1973) 1425
6. A.K. Sinha, B.C. Giessen and D.E. Polk in Treatise on Solid state chemistry, Vol. 3, N.B.Hanny, ed.Plenum Press, New York., 1976, p. 1.
7. C.P. Chou, L.A. Davies and R. Hasegawa, J. Appl. Phys. 50, (1979) 3334
8. L.A. Davies, R. Ray, C.P. Chou and R.C. O. Handley, Scripta. Met., 10, (1976) 541.
9. R. Ray and L. Tanner, Mater. Sci. Eng., 45, (1980) 195.
10. F.E. Luborsky, Proc. Second Int. Conf. on Amorphous Magnetism, R.A. Levy and R. Hasegawa eds. Plenum Press, New York, Chapter XI.
11. K. Hashimoto and T. Masumoto, in Proc. Second. Int. Conf. on Rapidly quenched Metals, Section II, N.J. Grant and B.C. Giessen eds., Mater. Sci. Eng. 23, (1976) 285.
12. G.O. Jones, Glass, Chapmen and Hall, London (1971)
13. F.E. Luborsky, Mater. Sci. Engg. 28, (1977) 139.
14. J.R. Matey and A.C. Anderson, J. Non. Cryst. Solids, 23, (1977) 129.

15. J. Logan and M.F. Ashby, Acta Metall. 22 (1974a) 1074.

16. R. Maddin and T. Masumoto, Mater. Sci. Eng., 9 (1972) 153

17. T. Murata, H. Kimura and T . Masumoto, Scr. Metall. 10, (1976) 705.

18. T.D. Hadnagy, D.J. Krenisky and T. Masumoto, Scr. Metall, 12, (1978) 45.

19. H.S. Chen. and D. Turnbull, J. Chem. Phys. 48, (1968) 2560

20. H.S. Chen and M. Gold Stain, J. Appl. Phys. 43, (1971) 1642

21. T. Egami, Mat. Res. Bull. 13, (1980) 557.

22. E.A. Chakachery, Fabrication and Characterization of Iron-Boron Metalic Glass Ribbons, M.Tech. Thesis, I.I.T. Kanpur, P. 23.

23. D.E. Polk and D. Turnbull, Acta Met. 20 (1972) 493.

24. D.S. Boudrean and J.M. Gregor, J. Appl. Phys. 48 (1977) 5057

25. H.S. Chen. J. Non Cryst. Solids 27 (1978) 257.

26. J. Magusav, A.S. Argon and N.J. Grant, Proce. Third Int. Conf. on Rapidly Quenched Metals, P. 392, Metals Society, Brihgton, England (1978) Mater. Sci. Engg. 38 (1979) 63.

27. T. Masumoto, Acta. Met. 19 (1971) 725.

28. H.J. Leany, H.S. Chen and T.T. Wang, Met.Trans. 3 (1972) 699

29. C.A. Pampillo and D.E. Polk, Acta. Met. 22 (1974) 741

30. C.P. Chou and F. Spaepen, Acta met. 23 (1975) 609.

31. C.A. Pampillo and A.C.Reimsch Vessel. J. Mat. Sci. 97 , (1974) 18

32. A.I. Taub and F. Spaepen, Scripta. Metall. 13, (1979) 195.

33. J.C. Gibeling and W.D. Nix, Scripta. Metall, 12 (1978) 919

34. C. Horner and A. Eberhardt, Scripta. Metall. 14, (1980) 1331.

35. P. Patterson and D.R.H. Johes, Acta Metall, 28 (1960) 675

36. D.G. Ast. and D.J. Kvenitssky, J. Mater. Sci. 14 (1979) 287

37. H. Eyring, I, Chem. Phys. 4 (1936) 283.

38. F. Sapepen, Acta. Metall 25 (1977) 407.

39. A.S. Argon, Acta. Metall, 27 (1979) 47

40. A.I. Taub, Acta. Matall, 30 (1982) 2117

41. D. Lee, Metall, Trans. 12 (1980) 419

42. A.I. Tomb and F. Spaepen, Acta. Metall, 28 (1980) 1781

43. H.S. Chen. Rep. Prog. Phys. 4 (1980) 353

44. A.I. Taub and F. Spaepen, J. Mat. Sci. 16 (1981) 3087.

45. F. Spaepen and D. Turnbull in J.J. Gilman and H.Leamy (eds.) Metallic glasses, Americal Society for Metals, Metals Park OH1978 p. 114.

46. A.I. Taub and F. Spaepen, Ser. Metall. 14 (1980) 1197

47. S.S. Tsao and F. Spaepen in T. Masumoto and K. Suzuki (eds) Proc. 4th. Int. Conf. on Rapidly quenched metals, Sendai, August 1981, Japan Institute of Metals, Sendai, 1981 p.463.

48. G.H. Vineyard, J. Phys. Chem Solids 3 (1957) 121

49. J.C. Li in T. Masumoto and K. Suzuki (eds.) Proc. 4th. Int. Conf. on Rapidly Quenched metals, Sendai,August 1981, Japan Inst. of Metals, Sendai, 1981 p. 1335.

50. A.I. Taub, Acta. Metall, 28 (1980) 633

51. A.I. Taub, and F.E. Loborsky, Acta. Metall 29 (1981) 1939.

52. H. Kronmuller, J. Phys. 41 (1980) C8 - 618.

53. G. Schroeder, R. Schafer and H. Kronmuller, Physics Status Solids, 50 (1978) 475.

54. J.J. Becker, AID Conf. Proc. 29 (1976) 204.

55. T. Takamosi, T. Misogushi and T.R. McGuire, Mater. Res. Bull. 15 (1980) 81.

56. A.I. Taub, Acta. Metall, 30 (1982) 2129

57. A.I. Taub, and F.E. Loborsky, Mat. Sci. Eng. 56 (1982) 157

58- N.S. Kazama, M Mitera and T. Masumoto in B. Cantor ed. Proc. 3rd. Int. Conf. on Rapidly Quenched Metals, Brighton, Vol. 2, Metal Society 1978 p. 164.

59. M. Mitera and T. Masumoto, Unpublished data.

60. M.Hagiwara, A. Inoue and T. Masumoto. Annu. Meet of Japan Inst. of Metals, 1980.

61. K. Hoselitz, Proc. Second Int. Cong. Rapidly quenched metals, Metals Society Brighton, England, P. 245.

62. F.A. Mecleintok and A.S. Argon, Mechanical Behaviour of Metals Chap. 7. Addision Wesiely, Reading Mass (1966).

63. J. Walter and F.E. Luborsky, Mat. Sci. Engs. 35 (1978) 255.

APPENDIX

Transition state theory predicts that

$$\dot{\gamma} = \dot{\gamma}_o \sin h \frac{\tau \gamma_o \Omega_f}{KT}$$

A fit of this equation to the equivalent shear strain rate - equivalent shear stress data points was attempted as follows.

Least square error = $e = \sum (\dot{\gamma}_i - \dot{\gamma}_o \text{ Sin h } \frac{\tau_i \gamma_o \Omega_f}{KT})^2$ ..A.I

Differentiating with respect to $\dot{\gamma}_o$ we get

$$\frac{\partial e}{\partial \dot{\gamma}_o} = \sum 2(\dot{\gamma}_i - \dot{\gamma}_o \sin h \frac{\tau_i \gamma_o \Omega_f}{KT})(- \sin h \tau_i \frac{\gamma_o \Omega_f}{KT})$$

For minimising the error function

$$\frac{\partial e}{\partial \dot{\gamma}_o} = 0$$

$$\sum \dot{\gamma}_i \sin h \tau_i \frac{\gamma_o \Omega_f}{KT} = \dot{\gamma}_o \sum \sin h^2 \tau_i \frac{\gamma_o \Omega_f}{KT}$$

$$\dot{\gamma}_o = \frac{\sum_{i=1}^{n} \dot{\gamma}_i \sin h \frac{\tau_i \gamma_o \Omega_f}{KT}}{\sum_{i=1}^{m} \sin h^2 \tau_i \frac{\gamma_o \Omega_f}{KT}} \quad \text{.....A II}$$

$$\frac{\partial e}{\partial \dot{\gamma}_o \Omega_f} = \sum 2(\dot{\gamma}_i - \dot{\gamma}_o \sinh \tau_i \frac{\gamma_o \Omega_f}{KT}) \cdot (\dot{\gamma}_o \cosh \tau_i \frac{\gamma_o \Omega_f}{KT}) \cdot (\frac{\tau_i}{KT}) = 0$$

Substituting for ϑ_o from A II,

$$E = \sum \gamma_i \tau_i \cosh\left(\frac{\tau_i \vartheta_o \Omega_f}{kT}\right) \cdot \left(\frac{\sum \gamma_i \sinh \frac{\tau_i \gamma_o \Omega_f}{kT}}{\sum \sinh^2 \frac{\tau_i \vartheta_o \Omega_f}{kT}}\right)$$

$$\frac{1}{2} \sum \tau_i \sinh^2\left(\frac{\tau_i \Omega_f \vartheta_o}{kT}\right) \cdot \left(\frac{\sum \vartheta_i \sinh \frac{\tau_i \gamma_o \Omega_f}{kT}}{\sum \sinh^2 \frac{\tau_i \vartheta_o \Omega_f}{kT}}\right)^2$$

This E must be minimised in order to fix a value of $\vartheta_o \Omega_f$

$$\therefore \dot{\vartheta}_o \Omega_f = \gamma_o \Omega_f + E .$$

In the present case, $\vartheta_o \Omega_f$ is of the order of 10^{-30} while the mimimum error value E was calculated to be of the order of 10-

Hence, during the subsequent calculations, there was overflow in sin h, sin 2h functions and hence this fit coult not be carried out.